

Manuscript version: Author's Accepted Manuscript

The version presented in WRAP is the author's accepted manuscript and may differ from the published version or Version of Record.

Persistent WRAP URL:

<http://wrap.warwick.ac.uk/138543>

How to cite:

Please refer to published version for the most recent bibliographic citation information. If a published version is known of, the repository item page linked to above, will contain details on accessing it.

Copyright and reuse:

The Warwick Research Archive Portal (WRAP) makes this work by researchers of the University of Warwick available open access under the following conditions.

Copyright © and all moral rights to the version of the paper presented here belong to the individual author(s) and/or other copyright owners. To the extent reasonable and practicable the material made available in WRAP has been checked for eligibility before being made available.

Copies of full items can be used for personal research or study, educational, or not-for-profit purposes without prior permission or charge. Provided that the authors, title and full bibliographic details are credited, a hyperlink and/or URL is given for the original metadata page and the content is not changed in any way.

Publisher's statement:

Please refer to the repository item page, publisher's statement section, for further information.

For more information, please contact the WRAP Team at: wrap@warwick.ac.uk.

Connections of the human orbitofrontal cortex and inferior frontal gyrus
Cerebral Cortex 2020 doi 10.1093/cercor/bhaa160

Chih-Chin Heather Hsu¹, Edmund T. Rolls^{2,3,4,*}, Chu-Chung Huang², Shin Tai Chong⁵, Chun-Yi Zac Lo², Jianfeng Feng^{2,3,*}, Ching-Po Lin^{1,2,5,6,*}

1. Department of Biomedical Imaging and Radiological Sciences, National Yang-Ming University, Taipei, Taiwan
2. Institute of Science and Technology for Brain Inspired Intelligence, Fudan University, Shanghai, China
3. Department of Computer Science, University of Warwick, Coventry, UK
4. Oxford Centre for Computational Neuroscience, Oxford, UK
5. Institute of Neuroscience, National Yang-Ming University, Taipei, Taiwan
6. Brain Research Center, National Yang-Ming University, Taipei, Taiwan

*Corresponding author information:

Professor Edmund T. Rolls,

Department of Computer Science, University of Warwick, Coventry CV4 7AL, UK.

Email: Edmund.Rolls@oxcns.org

URL: <https://www.oxcns.org>

orcid.org/0000-0003-3025-1292

Professor Jianfeng Feng,

Institute of Science and Technology for Brain-inspired Intelligence, School of Mathematical Sciences, Fudan University, Shanghai 200433, China,

Department of Computer Science, University of Warwick Coventry CV4 7AL, UK.

Email: jianfeng64@gmail.com

Professor Ching-Po Lin,

Institute of Neuroscience, National Yang-Ming University, Taipei, 11221, Taiwan,

Institute of Science and Technology for Brain-inspired Intelligence, School of Mathematical Sciences, Fudan University, Shanghai 200433, China.

Email: chingpolin@gmail.com

Abstract

The direct connections of the orbitofrontal cortex were traced with diffusion tractography imaging and statistical analysis in 50 humans, to help understand better its roles in emotion and its disorders. The medial orbitofrontal cortex and ventromedial prefrontal cortex have direct connections with the pregenual and subgenual parts of the anterior cingulate cortex, all of which are reward-related areas. The lateral orbitofrontal cortex (OFClat), and its closely connected right inferior frontal gyrus (rIFG), have direct connections with the supracallosal anterior cingulate cortex, all of which are punishment or non-reward-related areas. The OFClat and rIFG also have direct connections with the right supramarginal gyrus and inferior parietal cortex, and with some premotor cortical areas, which may provide outputs for the OFClat and rIFG. Another key finding is that the ventromedial prefrontal cortex shares with the medial orbitofrontal cortex especially strong outputs to the nucleus accumbens and olfactory tubercle, which comprise the ventral striatum, whereas the other regions have more widespread outputs to the striatum. Direct connections of the orbitofrontal cortex and IFG were with especially the temporal pole part of the temporal lobe. The left IFG, which includes Broca's area, has direct connections with the left angular and supramarginal gyri.

Keywords: orbitofrontal cortex; inferior frontal gyrus; diffusion tractography imaging; connections; emotion

The orbitofrontal cortex (OFC), is a key brain region involved in emotion (Rolls 2014, 2019b). Part of its importance in emotion is that the human orbitofrontal cortex encodes reward value and pleasantness in the medial orbitofrontal cortex, and punishment value, unpleasantness, and non-reward in the lateral orbitofrontal cortex (Rolls 2019c). The ventromedial prefrontal cortex is also involved in emotion, and may be especially involved in emotion-related decision-making, based on activations in it during reward-related decision-making (Rolls and Grabenhorst 2008; Rolls et al. 2010b, 2010a; Grabenhorst and Rolls 2011), and the effects of damage to it on decision-making (Hornak et al. 2004; Wheeler and Fellows 2008; Glascher et al. 2012). It is important to understand the functioning of these regions better, for all are implicated, in different ways, in depression by their altered functional connectivity (Cheng et al. 2016; Cheng et al. 2018b; Cheng et al. 2018c; Cheng et al. 2018d; Rolls et al. 2020a). Further, in depression, at least the orbital part of the right inferior frontal gyrus has similarly altered functional connectivity to that of the immediately adjacent lateral orbitofrontal cortex (Rolls *et al.* 2020a).

To understand the function of a brain region, it is very important to know where it receives its inputs from, and where it projects to (Rolls 2016a, 2021). There is a wealth of evidence on this in non-human primates, in which anatomical pathways can be traced (Carmichael and Price 1996; Price 2006; Price 2007; Saleem et al. 2008; Saleem et al. 2014). However, these methods cannot be applied in humans, and there is little evidence on the direct connections of the orbitofrontal cortex, ventromedial prefrontal cortex, and inferior frontal gyrus in humans. Some of the evidence available on the connectivity of these regions in humans comes from studies of functional connectivity (Du et al. 2020). Functional connectivity, measured by correlations in the BOLD signal between pairs of brain regions, does reflect direct connections as shown by combined anatomical and functional connectivity studies in non-human primates, but also reflects trans-synaptic effects (Van Essen et al. 2019).

Given this background, the aim of the present investigation was to use diffusion tractography imaging to investigate the direct connections of the human orbitofrontal cortex, ventromedial prefrontal cortex, and inferior frontal gyrus. These three brain regions were all included in this investigation because parts of all of them are related to emotion and depression (Rolls 2019b, 2019c; Rolls *et al.* 2020a), and we wished to know to what extent different parts of these areas have related or different connectivity. Diffusion tractography imaging, which is a MRI method that can probe direction-dependent diffusivity of water molecules in fibre bundles, can provide evidence on direct connections between brain regions (Mori and van Zijl 2002; Johansen-Berg et al. 2005; Donahue et al. 2016). Some previous studies have used tractography to investigate the connectivity of some limbic areas (Catani et al. 2013; Folloni et al. 2019)

including the subgenual cingulate cortex (Johansen-Berg et al. 2008), but this is the first study we know to focus on the human orbitofrontal cortex, ventromedial prefrontal cortex, and inferior frontal gyrus; to include a large number (N=50) of participants in such a study to allow statistical evaluation of the connections of these brain areas with all other areas of the cerebrum; and to analyze the results in a way that facilitates comparison with the functional connectivity of the same brain areas (Du *et al.* 2020). We emphasize that this is a voxel-level direct connectivity study, but a feature is that the regions are identified by the automated anatomical labelling atlas 3 (AAL3), which has a useful parcellation of both the orbitofrontal and anterior cingulate cortices (Rolls et al. 2015; Rolls et al. 2020b).

Methods

Participants

Data from 50 healthy aging participants (M/F = 19/31, mean age = 64.3±6.0, education = 14.6±2.8 year) from the Longitudinal Aging Study of Taipei (LAST) were analyzed in this study. LAST is a community-based aging cohort study conducted in Taipei and new Taipei city of Taiwan. The inclusion criteria for LAST participants were: (1) inhabitants of Taipei or new Taipei city without a plan to move in the near future, and (2) residents aged 50 years or older. People with the following conditions were excluded: (1) unable to communicate and complete an interview, (2) unable to complete all tests due to poor functional status, (3) those who had a limited life expectancy due to major illnesses, (4) those who were currently institutionalized. All participants signed a written informed consent agreement before they were enrolled for study. The study was approved by the Institutional Review Board of the National Yang Ming University, Taipei, Taiwan. All participants received the Montreal Cognitive Assessment (MoCA) for the global cognitive functional neuropsychological assessment, which is an alternative for the Mini-Mental State Exam (MMSE) that better identifies cognitive deficits in participants over 60 years old than MMSE (Nasreddine et al. 2005). MoCA scores range between 0 and 30. A score of 26 or over is considered to be normal. In this study, the participants' average MoCA score was 27.64±1.92 (± sd).

MRI Acquisition

All neuroimaging was performed on a 3T MR scanner (Siemens Magnetom Tim Trio, Erlangen, Germany) at the National Yang-Ming University, using a 12-channel head array coil. High-resolution T1-weighted (T1W) MR images were acquired using a 3D Magnetization-Prepared RApid Gradient Echo (3D-MPRAGE) sequence (TR/TE = 2530/3.5 ms, TI = 1100 ms, FOV = 256 mm, flip angle = 7°, matrix size = 256 x 256,

192 sagittal slices, slice thickness = 1 mm, no gap) for image segmentation, registration, and brain mask extraction. Multi-shelled, multi-band diffusion weighted images (DWI) were acquired using a single shot spin-echo planar imaging (EPI) sequence (monopolar scheme, TR = 3525 ms, TE = 109.2 ms, Matrix size: 110x110, voxel size: 2 x 2 x 2 mm³, multiband factor = 3, phase encoding: anterior to posterior) with two b-values of 1000 s/mm² (30 diffusion directions) and 3000 s/mm² (60 diffusion directions), in which b0 images were interleaved in every 6 volumes. Each volume consisted of 72 contiguous axial slices (thickness: 144 mm). Data with the same DWI protocol using an opposite polarity (phase encoding from posterior to anterior) were also acquired.

Diffusion MRI Preprocessing and Tractography

To correct for susceptibility-induced off-resonance field, image distortion induced by the fast-switching gradient, and slight head motion, FSL functions: TOPUP and EDDY were performed on diffusion weighted images with two opposite polarities (anterior and posterior). To reconstruct white matter tracts by using tractography imaging, T1W images were firstly segmented into five tissue types, using 5TT (MRtrix3 command: 5ttgen) including cortical gray matter (GM), subcortical gray matter, white matter (WM), cerebrospinal fluid, and pathological tissue, in order to anatomically constrain the tractography terminations in gray matter. Whole brain tractography was reconstructed for each subject in native space. A Multi-Shell Multi-Tissue Constrained Spherical Deconvolution (MSMT-CSD) model with lmax=8 and prior co-registered 5tt image was used on the preprocessed_multi-shell DWI data to obtain the fibre orientation density (FOD) function (Smith 2002; Jeurissen et al. 2014). Based on the voxel-wise fibre orientation distribution, anatomically-constrained tractography (ACT) using the iFOD2 algorithm was applied with random seeding of all WM voxels (20 seeds per voxel) to explore all possible connections without using a prior ROI for a hypothesis (Tournier et al. 2010; Smith et al. 2012). Placing seeds throughout the WM mask guaranteed that the reconstructed fibres would cover the whole of WM, and that WM seeding captures more underlying streamlines between regions than seeding in a GM ROI (Zajac et al. 2017). To enhance the validity of the reconstructed fibres, the aforementioned 5TT was utilized as prior information during the tracking, and six mandatory rules were applied: 1) A streamline was terminated and accepted when it entered GM. 2) A streamline was rejected if it entered CSF. 3) A streamline was terminated and accepted if it left the FOV or user-defined brain mask. (This is necessary to permit tracts to include the spinal column.) 4) A streamline was terminated and rejected when it reached a voxel with a very low FOD amplitude or showed excessive curving angle in the WM (with default threshold: FOD amplitude 0.05 and curve angle 45°). 5) A streamline was accepted when rule (4) applied within

subcortical regions. 6) A streamline was not allowed to exit subcortical GM and was truncated when it reached a minimum FOD amplitude within voxels of the subcortical GM (Smith *et al.* 2012). Whole-brain tractography was used for connectome reconstruction. To show the connectivity pattern of a ROI based on this voxel-to-voxel level connectivity, we included all voxel-to-voxel streamlines that terminated in the ROI.

In this study, we used the automated anatomical labelling atlas 3 (AAL3) (Rolls *et al.* 2020b) (see Tables S1 and S2 for description and abbreviations) to delineate individual brain areas of interest, because it has several divisions of the anterior cingulate cortex, as well as of the orbitofrontal cortex areas introduced in AAL2 (Rolls *et al.* 2015). To transform the AAL3 atlas from MNI standard space to the individual native space, T1W images were firstly co-registered with null diffusion images ($b = 0$) using boundary-based registration (BBR) to generate the transformation matrix from DWI-space to T1-space (Greve and Fischl 2009). Secondly, T1W images were then spatially normalized to the MNI152 T1 template in standard space via linear affine transformation (FLIRT) and non-linear registration (FNIRT) (Jenkinson and Smith 2001; Jenkinson *et al.* 2002). By combining the two transformation matrices (DWI to T1 and T1 to MNI), we then applied the inverse transformation matrix to obtain the AAL3 volumes in each individual's native DWI space with nearest neighbor interpolation. All the spatial registration and normalization procedures were implemented in FMRIB's Software Library (FSL, <http://www.fmrib.ox.ac.uk/fsl>). In this study, we focused on the connectivity of eight Regions of Interest (ROIs) which were defined by 18 AAL3 areas as shown in Fig. 1 as follows, separately for the left and right: the ventromedial prefrontal cortex (vmPFC, AAL3 FrontalMedOrb); medial orbitofrontal cortex (medOFC, AAL3 OFCpost, OFCant, OFCmed, rectus); lateral orbitofrontal cortex (latOFC, AAL3 OFClat, IFGorb); and inferior frontal gyrus (IFG, IFGtri, IFGoperc). The left and right were analysed separately, because there is evidence supporting asymmetry of the connectivity in the left and right IFG (Du *et al.* 2020), and to provide evidence on the extent to which each of the ROIs has bilateral connections. To reduce potential false positive tracts generated by seeding in only a few specific regions, whole-brain tractography was performed and the connectivity profiles of the regions of interest were then extracted. With the native-space AAL3 atlas, we used the `tck2connectome` command to generate the connectivity matrix for whole-brain tractography, in which a 2 mm radial search was applied to each streamline endpoint to locate the nearest node. The number of streamline fibres between pairs of AAL3 brain regions was measured across the 140 brain regions (the 26 regions of the cerebellum were omitted from the analyses). The number of streamlines between brain regions was then normalized by the average size (number of voxels) of each ROI pair

to reduce the bias toward capturing more streamlines between large ROI pairs. Thus, the connectivity for different ROI pairs was evaluated by the normalized number of streamlines (fibres per voxel). This enabled us to produce a matrix of the connectivity between each of the orbitofrontal cortex / inferior frontal gyrus ROIs and every other AAL3 area. (An example is in Fig. 4).

To establish the termination map of streamline tracts throughout the brain for individual subjects, we extracted the coordinates of every fibre termination identified for each of the eight ROIs, and recorded the number of connections to obtain the voxel-wise connection patterns in native space. The native termination maps were then warped into the MNI standard space for further representation and statistical analyses. (Examples of such maps are shown in Figs. 2 and S1.)

Statistics

To investigate the connectivity patterns of fibre projections between each of the 18 AAL3 areas in the eight ROIs [left and right: vmPFC (AAL3 FrontalMedOrb), medial OFC (Rectus, OFCmed, OFCant and OFCpost), lateral OFC (OFClat and IFGorb), and Inferior Frontal Gyrus (IFGoperc and IFGtri)] and each AAL3 region throughout the brain, the following statistical analysis was performed. For each of the 50 participants, the background level of normalized streamlines between each of the 18 AAL3 areas and each of the early visual cortical areas was measured. The early visual areas, Calcarine to OccipitalInf in the AAL3 atlas (AAL3 47-58), were used as control regions, because based on known anatomy in macaques (Carmichael and Price 1996; Price 2006; Price 2007; Saleem *et al.* 2008; Saleem *et al.* 2014), there are unlikely to be direct connections between these orbitofrontal cortex regions of interest and early visual cortical areas. The mean background level across visual cortical areas provided a background measure for each of the 18 AAL3 areas for each participant. Then a paired t test was performed across the 50 subjects for each link between AAL3 regions and the 18 AAL3 areas in the four ROIs to test whether the normalized number of streamlines was greater than the baseline background measure, using Bonferroni correction (corrected p-value < 0.05) for multiple comparisons across all AAL3 areas (140). (This resulted in an analysis of the type illustrated in Figs. 4 and S2).

To show voxel-level connectivity patterns of the eight ROIs across the 50 participants, a paired t test was also used to examine whether the number of streamline terminations in each voxel was significantly greater than the mean number of terminations for the baseline background. Termination t maps in MNI standard space were generated for the voxel-wise connectivity of the eight ROIs, using a threshold t value for $p < 0.001$ uncorrected, to produce analyses of the type illustrated in Fig. 3.

Results

1. Connectivity of different regions of the orbitofrontal cortex and nearby areas for a typical single subject

We start by showing in Figs. 2 and S1 for two single subjects the streamline terminations throughout the brain for five different ROIs, the right ventromedial prefrontal cortex, right medial orbitofrontal cortex, right lateral orbitofrontal cortex, and left and right inferior frontal gyrus. Separate diagrams are provided for the left and right IFG because the connectivity of the IFG was asymmetric between the right and left hemispheres, whereas for the other brain regions, the connectivity was symmetric. The connectivity for each of these 5 brain regions is described next. We emphasize that this is a voxel-level connectivity study. The AAL3 atlas is used only to delineate areas to which we wish to refer. The AAL3 regions that were the origin/termination of the streamlines in the regions of interest are shown in Fig. 1. The streamlines for the second typical subject are shown in Fig. S1 to indicate the robustness even at the single subject level, are shown with more coronal slices, and are drawn on for the following description.

Ventromedial prefrontal cortex

Figs. 2A and S1A show the streamline terminations for the ventromedial prefrontal cortex. Terminations are evident in the frontal pole, lateral orbitofrontal cortex, medial orbitofrontal cortex, striatum (ventral striatum and parts of the caudate and putamen), temporal pole, dorsolateral amygdala (with the streamline terminations there at $Y=0$ probably indicating where the following of the streamlines terminates as bundles enter the amygdala), inferior temporal cortex (with sparse connectivity illustrated), and the posterior cingulate cortex (at $Y=-42$). We note that it is typically not possible to easily follow the streamline tracts from the white matter into the grey matter of the cortex itself because there are so many axons running tangentially just below layer 6 of the cortex, connecting to other cortical regions. These tangential fibres produce difficulty in following the diffusion-based process that is present in the streamlined fibres being traced (D. Van Essen, personal communication, Nov 2019).

Medial orbitofrontal cortex

Figs. 2B and S1B show the streamline terminations for the medial orbitofrontal cortex. Terminations are evident in the frontal pole, lateral orbitofrontal cortex, pregenual cingulate cortex (with less connectivity to the supracallosal anterior cingulate cortex), striatum (ventral striatum, caudate, and putamen), temporal pole, dorsolateral amygdala,

middle and inferior temporal gyrus, the posterior cingulate cortex (at $Y=-36$ to $Y=-48$), and precuneus ($Y=-48$ to $Y=-66$). Interestingly, some connectivity to contralateral orbitofrontal cortex areas is evident.

Lateral orbitofrontal cortex

Fig. 1C and S1C show the streamline terminations for the lateral orbitofrontal cortex. Terminations are evident in the frontal pole and dorsolateral prefrontal cortex, medial orbitofrontal cortex, inferior frontal gyrus, supracallosal anterior cingulate cortex ($Y=12$ to $Y=18$, with less connectivity to the pregenual cingulate cortex), anterior insula ($Y=12$ to $Y=18$), premotor cortex ($Y=0$ to $Y=6$), striatum (ventral striatum, caudate, and putamen), temporal pole, dorsolateral amygdala, inferior temporal cortex, the posterior cingulate cortex (at $Y=-36$ to $Y=-48$), and precuneus ($Y=-48$ to $Y=-66$), the angular gyrus (a $Y=-36$), and the MDm (the magnocellular part of the mediodorsal nucleus of the thalamus).

Left inferior frontal gyrus

Figs. 2D and S1D show the streamline terminations for the left inferior frontal gyrus. Terminations are evident in the frontal pole and superior, and middle frontal gyri, supracallosal anterior cingulate cortex ($Y=12$ to $Y=18$, with little connectivity to the pregenual cingulate cortex), anterior insula ($Y=12$ to $Y=18$), premotor cortex ($Y=0$ to $Y=6$), striatum (caudate, putamen, and ventral striatum), temporal pole, dorsolateral amygdala, inferior temporal (visual) cortex, superior temporal (auditory) cortex ($Y=-12$ to $Y=-24$), the posterior cingulate cortex (at $Y=-36$ to $Y=-48$), and precuneus ($Y=-48$ to $Y=-66$), the left supramarginal gyrus area 40 (at $Y=-36$), the left angular gyrus area 39 (at $Y=-60$ to $Y=-66$), parietal area 7 (at $Y=-36$), and the thalamus. It is notable that there was little connectivity with the medial orbitofrontal cortex, ventromedial prefrontal cortex, and pregenual cingulate cortex.

Right inferior frontal gyrus

Figs. 2E and S1E show the streamline terminations for the right inferior frontal gyrus. Terminations are evident in the frontal pole and superior, and middle frontal gyri, lateral orbitofrontal cortex ($Y=30$), supracallosal anterior cingulate cortex ($Y=12$ to $Y=30$, with little connectivity to the pregenual cingulate cortex), anterior insula ($Y=12$ to $Y=18$), premotor cortex ($Y=0$ to $Y=6$), striatum (caudate, putamen, and ventral striatum), temporal pole, dorsolateral amygdala, inferior temporal (visual) cortex, middle temporal gyrus, superior temporal (auditory) cortex ($Y=-12$ to $Y=-24$), the posterior cingulate cortex (at $Y=-36$ to $Y=-48$), and precuneus ($Y=-48$ to $Y=-66$), the right supramarginal gyrus area 40 (at $Y=-36$), the right angular gyrus area 39 (at $Y=-60$

to $Y=-66$), parietal area 7 (at $Y=-36$), and the thalamus. It is notable that there was little connectivity with the medial orbitofrontal cortex, ventromedial prefrontal cortex, and pregenual cingulate cortex.

2. The statistics of the connectivity of the orbitofrontal cortex and related ROIs with voxels in other brain regions analyzed across 50 participants

Fig. 3 shows t maps from all 50 subjects to illustrate the strength of the connectivity of the orbitofrontal cortex and related areas with other brain regions, as described in the Methods. Termination maps were examined using a one-sample t test with a statistical threshold of $p<0.001$ uncorrected as described in the Methods.

Ventromedial prefrontal cortex

Fig. 3A shows the t maps for the streamline terminations for the ventromedial prefrontal cortex. The terminations are most significant in the frontal pole, lateral and medial orbitofrontal cortex, pregenual and subgenual cingulate cortex, striatum (ventral striatum, caudate, and putamen), temporal pole, dorsolateral amygdala, and the MDm (the magnocellular part of the mediodorsal nucleus of the thalamus).

Medial orbitofrontal cortex

Fig. 3B shows the t maps for the streamline terminations for the medial orbitofrontal cortex. The terminations are most significant in the frontal pole, lateral orbitofrontal cortex, pregenual cingulate cortex ($Y=30$, with less connectivity to the supracallosal anterior cingulate cortex), striatum (ventral striatum, caudate, and putamen), temporal pole and inferior temporal cortex, dorsolateral amygdala, a region close to where connections may enter the hippocampal formation ($Y=-12$), and the MDm (the magnocellular part of the mediodorsal nucleus of the thalamus).

Lateral orbitofrontal cortex

Fig. 3C shows the t maps for the streamline terminations for the lateral orbitofrontal cortex. The terminations are most significant in the frontal pole, medial orbitofrontal cortex, anterior insula ($Y=12$ to $Y=18$), striatum (caudate, putamen, and ventral striatum), temporal pole and inferior temporal cortex, dorsolateral amygdala, the supramarginal gyrus (at $Y=-36$), and the MDm (the magnocellular part of the mediodorsal nucleus of the thalamus).

Left inferior frontal gyrus

Fig. 3D shows the z maps for the streamline terminations for the left inferior frontal gyrus. The terminations are most significant in the frontal pole and superior, and

middle frontal gyri, supracallosal anterior cingulate cortex (Y=12 to Y=18, with little connectivity to the pregenual cingulate cortex), anterior insula (Y=12 to Y=18), premotor cortex (Y=0 to Y=6), striatum (caudate, putamen, and ventral striatum), temporal pole, dorsolateral amygdala, inferior temporal (visual) cortex, superior temporal (auditory) cortex (Y=-12 to -24), the left supramarginal angular gyrus area 40 (at Y=-36), the left angular gyrus area 39 (at Y=-60 to -66), parietal area 7 (at Y=-36), and the thalamus. It is notable that there was little connectivity with the medial orbitofrontal cortex, ventromedial prefrontal cortex, and pregenual cingulate cortex.

Right inferior frontal gyrus

Fig. 3E shows the z maps for the streamline terminations for the right inferior frontal gyrus. The terminations are most significant in the frontal pole and superior, and middle frontal gyri, right lateral orbitofrontal cortex (Y=30), supracallosal anterior cingulate cortex (Y=12 to Y=18, with little connectivity to the pregenual cingulate cortex), anterior insula (Y=12 to Y=18), premotor cortex (Y=0 to Y=6), striatum (caudate, putamen, and ventral striatum), temporal pole, right inferior temporal (visual) cortex, middle temporal gyrus, superior temporal (auditory) cortex (Y=-12 to Y=-24), the right supramarginal gyrus area 40 (at Y=-36), the right angular gyrus area 39 (at Y=-60 to -66), parietal area 7 (at Y=-36), and the thalamus. It is notable that there was little connectivity with the medial orbitofrontal cortex, ventromedial prefrontal cortex, and pregenual cingulate cortex.

3. The matrix of the connectivity of the eight orbitofrontal cortex and related areas

Fig. 4 shows a matrix of the connectivity measured across the 50 participants for the 18 AAL3 regions in the 8 ROIs (left and right vmPFC (FrontalMedOrb), medOFC (Rectus, OFCmed, OFCant and OFCpost), latOFClat (OFClat and IFGorb), and IFG (IFGoperc and IFGtri)) with other ipsilateral AAL3 brain regions. The connectivity of these 18 ROIs is typically greater ipsilaterally than contralaterally (with the contralateral connectivity shown in Fig. S2); and for most ROIs apart from the IFG the connectivity is approximately symmetric in the two hemispheres.

Fig. 4 (top row for the Left and Right connectivity matrices) shows that the ventromedial prefrontal cortex has strong direct connectivity with medial orbitofrontal cortex areas (especially with OFCmed and OFCpost), the caudate and putamen, the subgenual anterior cingulate cortex, temporal cortical areas, and some connectivity with superior and middle frontal gyri, the orbital part of the inferior frontal gyrus and lateral orbitofrontal cortex, and the insula.

The medial orbitofrontal cortex (AAL3 areas rectus, OFCmed, OFCant and OFCpost) have strong direct connectivity with the ventromedial prefrontal cortex,

striatum especially the ventral striatum, the anterior cingulate cortex especially the subgenual part, temporal cortical areas, and some connectivity with superior and middle frontal gyri and the orbital part of the inferior frontal gyrus. Differences between these AAL3 areas are that the OFCpost has especially strong connections with other parts of the medial orbitofrontal cortex (including rectus, OFCmed and OFC ant), with the vmPFC, with the orbital part of the inferior frontal gyrus (and the connected OFClat), and with the superior and middle frontal gyri. The OFC post is thus notable as being highly connected, like a hub. The rectus and OFCmed have especially strong connections with the nucleus accumbens and olfactory tubercle, which comprise the ventral striatum.

The lateral orbitofrontal cortex (AAL3 areas OFClat and IFGorb) has direct connectivity with the inferior frontal gyrus, superior, middle and medial superior prefrontal areas, the posterior orbitofrontal cortex, insula, caudate and putamen with less connectivity with the ventral striatum, temporal cortex, and supramarginal and inferior parietal cortical areas. The IFGorb has stronger connectivity with parietal areas than OFClat.

The right inferior frontal gyrus (AAL3 areas R.IFGoperc and R.IFGtri) has direct connections with many right prefrontal cortical areas, right premotor (precentral gyrus and supplementary motor area), postcentral cortex and midcingulate cortex, supracallosal anterior cingulate cortex, and right supramarginal, angular and inferior parietal cortical areas.

The left inferior frontal gyrus has direct connections with many left prefrontal cortical areas, left premotor, postcentral cortex and midcingulate cortex, supracallosal anterior cingulate cortex, and left supramarginal, angular and inferior parietal cortical areas.

The connections shown in Fig. 4 can be summarized in another way, by considering connectivities of OFC/IFG subregions with different brain systems. The temporal cortical areas are connected with all of these OFC/IFG regions. The parietal areas including the supramarginal, and angular gyri are connected especially with the inferior frontal gyri, and not with the orbitofrontal cortex and vmPFC. The IFGorb appears to have similarities with the other IFG areas and with the OFClat, and may be an intermediate area. The subgenual and pregenual anterior cingulate cortex tend to be connected with the medial OFC and vmPFC areas, whereas the supracallosal anterior cingulate cortex tends to be more connected with the inferior frontal gyrus areas including IFGorb. The posterior cingulate cortex and precuneus are especially connected with the vmPFC and the gyrus rectus. Motor areas, such as the precentral gyrus, supplementary motor area, rolandic operculum, and midcingulate cortex are connected with the IFG but much less with the OFC and vmPFC. The ventral striatum

(NAcc and olfactory tubercle) are connected especially with the medial OFC and vmPFC. The superior and middle frontal gyri appear to be connected at all OFC, vmPFC and IFG areas.

Fig. 5 shows the correlation between the connectivity of each of the 18 AAL3 areas with all ipsilateral AAL3 brain areas across 50 participants. The medial orbitofrontal areas rectus, OFCmed and OFCant, and the vmPFC form one group that have high correlations with each other. They have moderately high correlations with the pregenual and subgenual anterior cingulate cortex. Within this group, the vmPFC and gyrus rectus have especially strong correlations with the anterior cingulate cortex. The OFCpost forms a second group, and stands out as having connectivity that is different from most of these OFC, IFG and vmPFC areas, perhaps because it is a hub region. The OFClat and IFGorb form a third group, with connectivity correlated with that of medial OFC areas, which is not the case for the fourth group, IFGtri and IFGoperc. The fourth group, IFGtri and IFGoperc, have similar connectivity to parietal areas including the supramarginal and angular gyri and precuneus; to temporal lobe areas; to prefrontal areas including the superior and middle frontal gyri; and to some motor areas, including the precentral gyrus, supplementary motor area, Rolandic operculum, and mid-cingulate cortex. The connectivity of the lateral orbitofrontal cortex is correlated with that of the inferior frontal gyrus on the same side of the brain, and interestingly these connectivities had low correlations between the two hemispheres. This is an indication that the left and right lateral orbitofrontal may have different functions (Fig. S3). These groups defined by the correlations shown in Fig. 5 are of interest, for they help to define anatomical networks with similar connectivity (and implied interconnectivity within a network) in the human brain.

Fig. 6 shows a Multidimensional Scaling (MDS) space for the 18 AAL3 areas, based on their anatomical connectivity with AAL3 brain areas from Fig. S2. Fig. 6 is for when the AAL3 areas are from both hemispheres, and very similar results were found when the AAL3 areas were only from the ipsilateral hemisphere. Fig. 6 shows that the OFCmed, OFCant, gyrus rectus, and vmPFC are relatively close together in one part of the space, reflecting their similar connectivity with all AAL3 areas. The OFClat and IFGorb are relatively close to each other, indicating their similar connectivity to each other. Their position in the space is intermediate between the medial OFC areas and the IFG areas, which form a third part of the space. The OFCpost is separate in the space. This supports the points made when considering the results in Fig. 5 that there are four main groups of regions among the 18 AAL3 areas considered. The pattern of Left and Right anatomical connectivities is similar, as shown by the closeness of the Right and Left corresponding AAL3 areas in this space.

4. Tractography

We provide tractography diagrams for five regions of interest in the orbitofrontal cortex (Fig. S4), ventromedial prefrontal cortex, and inferior frontal gyrus of one representative participant. The overall pattern shows prominent inter-hemispheric connections of the five regions. The tractography for both the right and left IFG shows connections with the superior and middle temporal regions via the arcuate fasciculus.

Discussion

One key finding is that the human medial and lateral orbitofrontal cortex have different direct connections with other parts of the brain. The medial orbitofrontal cortex has direct connections with the anterior cingulate cortex including the pregenual and subgenual parts (Fig. 4), all of which are reward-related areas (Rolls 2019b, 2019c). The lateral orbitofrontal cortex has fewer connections with these parts of the anterior cingulate cortex, but the inferior frontal gyrus (which especially on the right is related to the lateral orbitofrontal cortex), has direct connections with the supracallosal anterior cingulate cortex (Fig. 4), all of which are punishment or non-reward-related areas (Rolls 2019b, 2019c). This extends the evidence from functional connectivity about the relations between these different parts of the medial orbitofrontal cortex vs lateral orbitofrontal cortex and its closely related right inferior frontal gyrus (Rolls et al. 2019; Du *et al.* 2020), by adding evidence about direct connections. This is consistent with the hypotheses that the orbitofrontal cortex computes reward value and thereby is related to emotion, and that the anterior cingulate cortex provides a route to goal-related actions (Rolls 2019a).

A second key finding is that the lateral orbitofrontal cortex and right inferior frontal gyrus direct connections are somewhat similar to each other, and somewhat different from medial orbitofrontal cortex areas, in terms of their direct connections with right hemisphere parietal areas such as the supramarginal gyrus and inferior parietal cortex (Fig. 4), and also some movement-related areas, such as the supplementary motor cortex. This is consistent with the hypothesis that the lateral orbitofrontal cortex and the associated right inferior frontal gyrus provide routes to behavioural output for the orbitofrontal cortex (Du *et al.* 2020) which have greater functional connectivity in depression (Rolls *et al.* 2020a). This extends the non-reward attractor theory of depression (Rolls 2016b) beyond the lateral orbitofrontal cortex to include at least parts of the right inferior frontal gyrus. A concept here is that with the involvement of the left inferior frontal gyrus in language (as Broca's area (Amunts and Zilles 2012; Clos et al. 2013)), the left orbitofrontal cortex becomes constrained in size, whereas the right inferior frontal gyrus can be more involved in functions of the right

orbitofrontal cortex, for which the right IFG may provide a route to output (Rolls *et al.* 2020a).

Another key finding is that the ventromedial prefrontal cortex shares with the medial orbitofrontal cortex especially strong outputs to the nucleus accumbens and olfactory tubercle, which comprise the ventral striatum, whereas the other ROIs have more widespread outputs to the striatum (Fig. 4). In macaques, the orbitofrontal cortex also projects to the ventral striatum (Selemon and Goldman-Rakic 1985; Yeterian and Pandya 1991; Haber *et al.* 1995; Haber 2016) (which helps to validate the current findings), but what is shown in Fig. 4 provides quantitative evidence for humans how this is especially the case for the vmPFC and medial orbitofrontal cortex, whereas the lateral orbitofrontal cortex and inferior frontal gyrus have relatively stronger connections with the caudate nucleus and putamen. The ventromedial prefrontal cortex like the medial orbitofrontal cortex also has strong direct connections with the anterior cingulate cortex, and indeed the connections with the subgenual and pregenual cingulate cortices distinguish these areas from the other ROIs.

As shown in Fig. 4 and summarized in the Results, the connections of the different OFC/IFG AAL3 areas form interesting anatomical groupings. We now show how these anatomical groupings have functional relevance. First, the medial orbitofrontal cortex has strong direct connectivity with the pregenual and subgenual anterior cingulate cortex, and both are implicated in reward processing (Grabenhorst and Rolls 2011; Rolls 2019b, 2019c). Conversely, the lateral orbitofrontal cortex has strong direct connectivity with the supracallosal anterior cingulate cortex (Fig. 4), and both are implicated in punishment and non-reward processing (Grabenhorst and Rolls 2011; Rolls 2019b, 2019c). This may be a network in which reward and punishment value is computed in the orbitofrontal cortex, and this information is sent to the anterior cingulate cortex for action to reward outcome learning (Rolls 2019a). The orbital part of the inferior frontal gyrus (IFGorb) appears to have similarities with both OFClat and the other IFG areas. On the right (*i.e.* contralateral to the language hemisphere), the orbital part of the inferior frontal gyrus appears to be functionally especially related to increased functional connectivity in depression, and may provide a route from the lateral orbitofrontal cortex to premotor areas (Cheng *et al.* 2016; Rolls *et al.* 2020a).

Second, the posterior cingulate cortex and precuneus are especially connected with the vmPFC and the gyrus rectus. This is especially interesting as both are related to memory, including autobiographical memory (Bonnici and Maguire 2018; McCormick *et al.* 2018). Consistent with this, the parahippocampal cortex, also with the hippocampus involved in memory (Rolls 2018), is especially connected with the vmPFC and gyrus rectus. Thus the vmPFC and gyrus rectus have connections in

humans that relates them to memory functions, and this may be a distinct system from the medial and lateral orbitofrontal cortex.

Third, the parietal areas including the supramarginal (BA40), and angular gyri (BA39) are connected especially with the inferior frontal gyri, and not with the orbitofrontal cortex and vmPFC. On the left, these are key areas involved with language, with the inferior frontal gyrus pars triangularis (BA45) and pars opercularis (BA44) forming Broca's area, and at least the angular gyri and related parieto-temporal areas involved in language and related processing (Amunts and Zilles 2012; DeWitt and Rauschecker 2013; Binder 2015; Campbell and Tyler 2018).

Fourth, motor areas, such as the precentral gyrus, supplementary motor area, Rolandic operculum, and midcingulate cortex are connected with the IFG but much less with the OFC and vmPFC. The ventral striatum (NAcc and olfactory tubercle) are connected especially with the medial OFC and vmPFC.

Fifth, the temporal cortical areas lobe had connections with all OFC, vmPFC and IFG areas. What was especially interesting, as shown in Figs. 2 and S1, is that the connections were especially strong with the temporal pole, though connections were also found less anteriorly. These temporal lobe regions are involved in visual (including face expression), auditory, and semantic functions (Patterson et al. 2007; Cheng et al. 2015; Rolls 2021). Consistent with the findings presented here for humans, in macaques the medial orbitofrontal cortex areas do have strong connectivity with the temporal pole (Corcoles-Parada et al. 2019), and the middle part of the superior temporal gyrus connects to the lateral orbitofrontal cortex area 12 and more laterally (Petrides and Pandya 1988). The superior and middle frontal gyri appear to be connected at all OFC, vmPFC and IFG areas, and these connections may be involved in working memory and executive function (Passingham and Wise 2012).

Sixth, as shown in Fig. 4, and supported by Figs. 5 and 6, the OFCpost is somewhat more connected than OFCant and other parts of the OFC, and appears to be a hub region. Differences are found in the architecture which for the posterior OFC is less elaborated than more anteriorly (Beck 1949; Barbas and Pandya 1989; Hof et al. 1995) and in macaques is related to different patterns of connections with anterior cingulate (Garcia-Cabezas and Barbas 2017) and other areas (Barbas 1993).

There is an interesting similarity between the direct connections of these ROIs (Figs 2 and 3) and their functional connectivity shown in Fig. 2 of Du et al (2020). Connectivity revealed by the functional connectivity but not by the direct connections include the angular gyrus with ventromedial prefrontal cortex, medial orbitofrontal cortex, and lateral orbitofrontal cortex (Du *et al.* 2020), and these therefore may be trans-synaptic connections. On the other hand, there is strong functional connectivity of the inferior frontal gyrus with the supramarginal gyrus (Fig. 2 of Du et al (2020)),

and that may be mediated by direct connectivity as shown in Fig. 4. In addition, it is interesting to compare Fig. 4 with a corresponding figure based on the functional connectivity of parcels within the orbitofrontal cortex and related ventromedial and inferior frontal gyrus brain areas (Fig. 4 of (Du *et al.* 2020)). Both Figures emphasise the differences of the connectivity of the vmPFC, medial orbitofrontal cortex, lateral orbitofrontal cortex, and inferior frontal gyrus.

An important guide to the connectivity of the human orbitofrontal cortex is the wealth of evidence available about the macaque orbitofrontal cortex (Carmichael and Price 1996; Price 2006; Barbas 2007; Price 2007; Saleem *et al.* 2008; Barbas *et al.* 2011; Saleem *et al.* 2014). However, the findings described here while generally consistent, go beyond those studies by providing evidence about the asymmetry of the human right and left lateral orbitofrontal cortex and inferior frontal gyri; by highlighting the connections of the human orbitofrontal cortex with parietal cortical areas some of which are involved in functions related to language; and in revealing the connectivity of the human medial orbitofrontal cortex with the pregenual cingulate cortex, and the lateral orbitofrontal cortex with the supracallosal anterior cingulate cortex, areas involved in humans respectively in reward vs punishment and non-reward processing (Rolls 2019a, 2019b, 2019c).

In relation to macaque anatomical studies, the connections shown in Fig. 4 are of interest, because they are based on a statistical analysis. This is in contrast to most anatomical studies in macaques, which are based essentially on several single case studies, in which particular case studies of injections into individual receiving areas (identified with retrograde tracers such as HRP) or sending areas (using anterograde tracers injected into a particular region) are performed. In contrast, in the present approach, and potentially in future approaches in humans, the anatomical connectivity can be based on statistical analyses of connectivity between voxels throughout the brain, which is essentially what happened in the present investigation, which then allows networks of connectivity to be defined, identified by statistical analysis, such as correlation as used here (Fig. 5), or potentially further approaches.

In order to obtain more precise fibre orientation estimates and more reliable tractography, the MSMT-CSD algorithm combined with ACT was used in this study (Smith *et al.* 2012; Jeurissen *et al.* 2014). However, there are still some limitations that may result in failing to identify particular connections. One limitation can arise for example when there are many tangential fibres to a pathway as described in the Introduction, as occurs for example in the dense white matter zone where axons run parallel to the cortical surface beneath the infragranular layer (Reveley *et al.* 2015; Donahue *et al.* 2016). Because much of the diffusion is in the tangential direction, it is difficult to follow orthogonal streamlines across this region penetrating into the cortex.

A similar issue may apply to orbitofrontal cortex connections with the amygdala, partly because there are many tangential fibres where the streamlines enter the amygdala, and partly because there may be a sharp turn in the streamlines at the entrance to the amygdala (Solano-Castiella et al. 2010) whereas most tracking algorithms favor the straight option (turning through an angle of less than 60 degrees) (Jeurissen et al. 2019). Thus, while the connectivity between the orbitofrontal cortex and amygdala has been well documented in functional connectivity and tracer studies (Carmichael and Price 1995; Ghashghaei and Barbas 2002; Barbas 2007; Garcia-Cabezas and Barbas 2017; Cheng et al. 2018a), it was hard to follow the streamlines into the amygdala in this study and in previous diffusion studies (Eden et al. 2015; Gibbard et al. 2018; Rizzo et al. 2018) (though streamlines terminating at the entrance to the amygdala are shown in Figs. 2 and 3). Nevertheless, although tractography needs to be treated with caution because of possible false negatives and positives, it has been the only methodology for non-invasively delineating the white matter pathways in the human brain. In this study, our purpose was not to provide a novel method to improve the tractography algorithm.

Instead, this study takes the orbitofrontal cortex and its related areas, parts of the brain important in emotion and in emotional disorders such as depression, and shows how these areas connect to other key brain regions, adding importantly to what can be assessed by anatomical path tracing studies in nonhuman primates, partly because some of the areas involved are much more developed in humans, including parts of the inferior frontal gyrus and the angular and supramarginal gyri. The present study also provides interesting evidence on the differences of connectivity of these brain regions, as described above. Moreover, this study provides a foundation for future longitudinal studies, and for studies in patients with disorders.

Funding

This work was supported as follows. CPL is supported by the Ministry of Science and Technology (MOST) of Taiwan (grant MOST 109-2634-F-010-001, MOST 108-2321-B-010-013-MY2, MOST 108-2321-B-010-010-MY2 and MOST 108-2420-H-010-001-); and National Health Research Institutes [grant NHRI-EX108-10611EI]. CYL was partially supported by the National Key Research and Development Program of China (No. 2018YFC0910503), the Young Scientists Fund of the National Natural Science Foundation of China (No. 81801774), and the Natural Science Foundation of Shanghai (No. 18ZR1403700). JF is supported by the key project of Shanghai Science and 480 Technology Innovation Plan (grant 16JC1420402), the Shanghai Municipal Science and Technology Major Project (No.2018SHZDZX01), ZJLab, National Key R&D Program of China (No.2018YFC1312900), and the 111 project (grant B18015).

Acknowledgements

This work was supported in part by the Brain Research Center, National Yang-Ming University from The Featured Areas Research Center Program within the framework of the Higher Education Sprout Project by the Ministry of Education (MOE) in Taiwan. The authors also acknowledge MRI support from the MRI Core of National Yang-Ming University, Taiwan.

Figures and Tables

Fig. 1. The four regions of interest (ROI), and the AAL3 areas included in each. The ventromedial prefrontal cortex ROI (vmPFC) is AAL3 area FrontalMedOrb; the medial orbitofrontal cortex ROI (medOFC) consists of AAL3 areas gyrus rectus, OFCmed, OFCant, and OFCpost; the lateral orbitofrontal cortex ROI (latOFC) consists of AAL3 OFClat and IFGorb; and the inferior frontal gyrus ROI (IFG) consists of AAL3 areas IFGtri (BA45) and IFGoperc (BA44). There is a close relation of these automated anatomical labelling 3 (AAL3) areas (Rolls *et al.* 2015; Rolls *et al.* 2020b) to the underlying cytoarchitecture (Öngür *et al.* 2003), with gyrus rectus corresponding to 14r; OFCmed to 13m; OFC post to 13l; OFCant to 11l; OFC lat to 12; OFGorb to the inferior frontal convexity which joins the lateral OFC 12 to the inferior frontal gyrus, 45; IFGtri to area 45; and IFGoperc to area 44. There is also a good correspondence of the AAL3 areas to the divisions of the orbitofrontal cortex based on parcellation of the functional connectivity (Du *et al.* 2020).

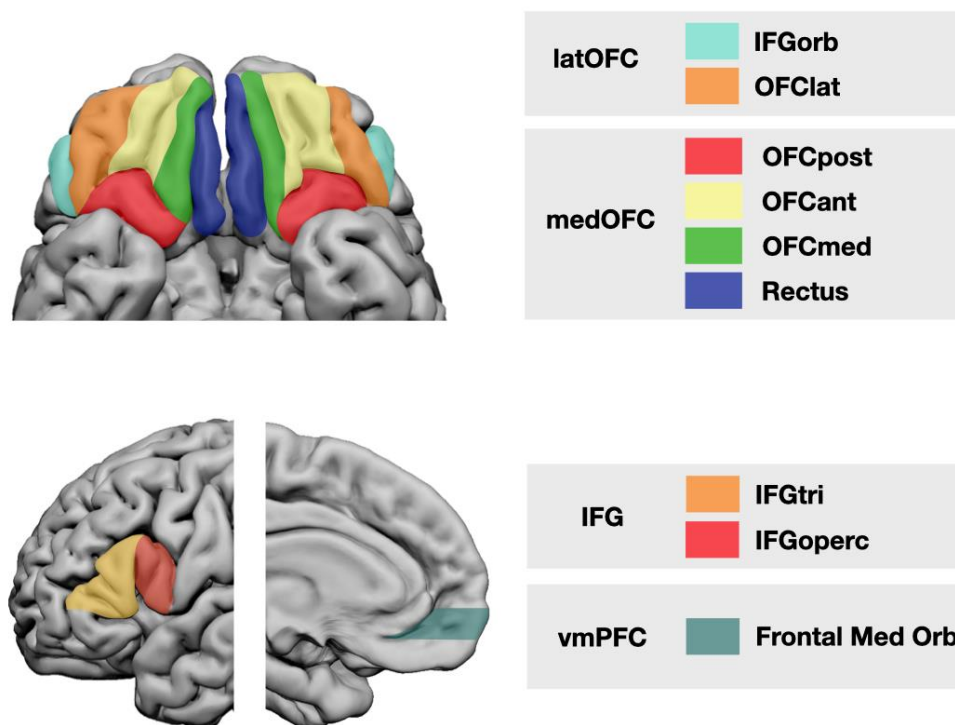


Fig. 2: The regions with streamline terminations for the connectivity of different regions of the orbitofrontal cortex and nearby areas for a typical single subject shown in MNI space. Separate sub-diagrams are provided for the (A) right ventromedial prefrontal cortex, (B) right medial orbitofrontal cortex, (C) right lateral orbitofrontal cortex, and (D) left and (E) right inferior frontal gyrus.

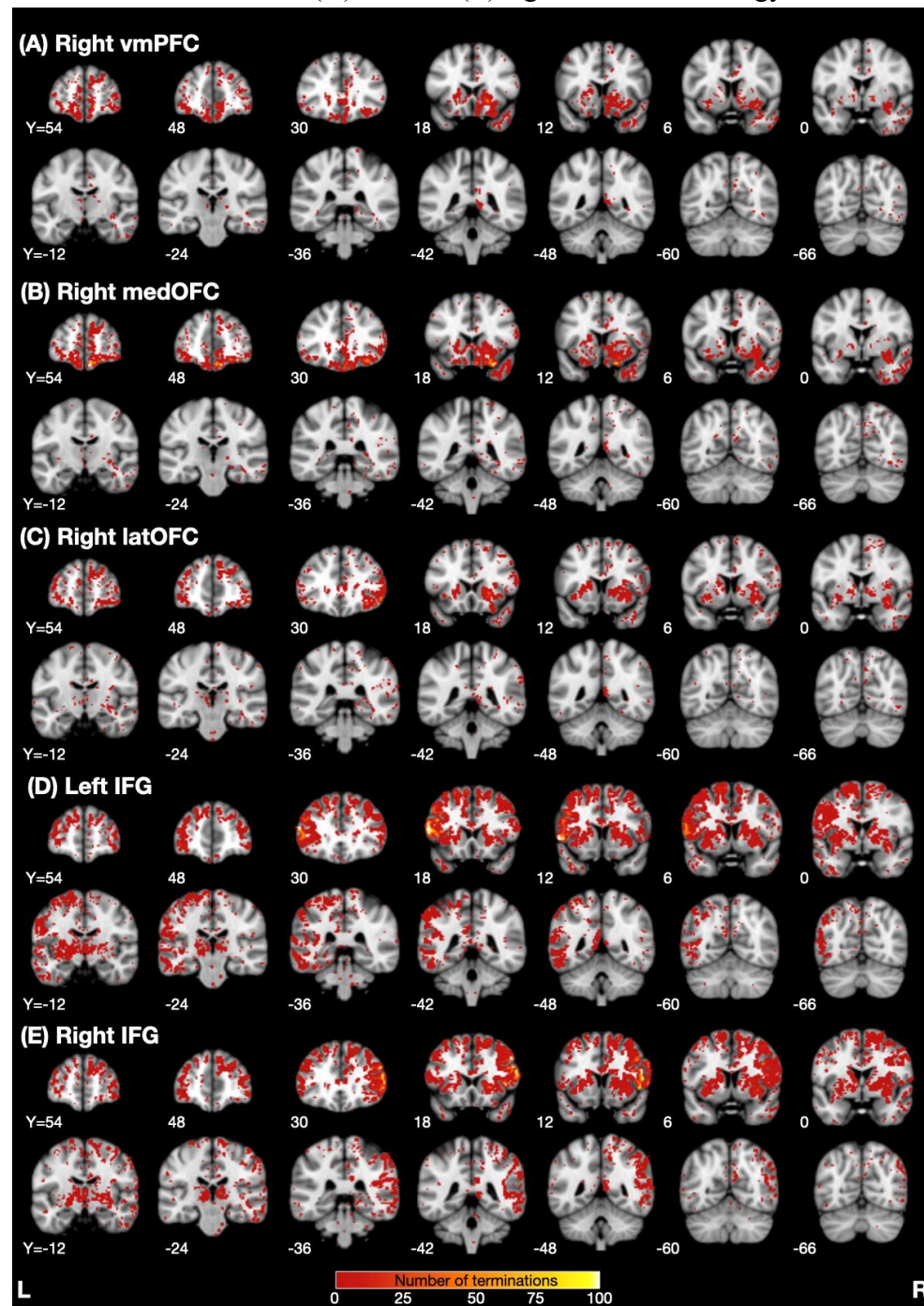


Fig. 3. t maps from all 50 subjects to illustrate the strength of the connectivity of the orbitofrontal cortex and related areas with other brain regions. Termination maps were examined by a voxel-wise paired t test using the mean termination numbers in the primary visual cortex as a baseline background measure with a statistical threshold of $p < 0.001$ uncorrected. Separate sub-diagrams are provided for (A) the ventromedial prefrontal cortex, (B) medial orbitofrontal cortex, (C) lateral orbitofrontal cortex, and (D) left and (E) right inferior frontal gyrus.

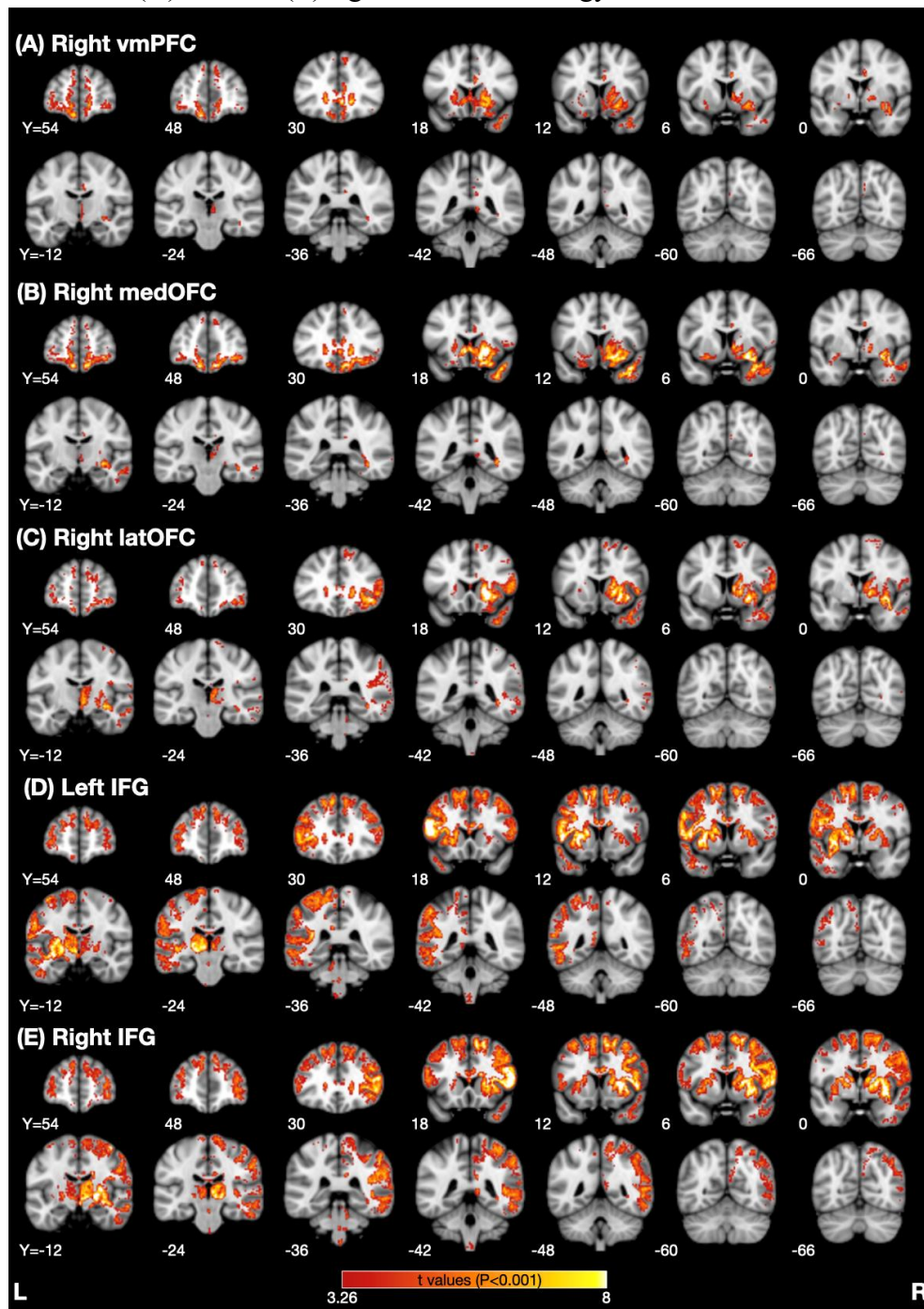


Fig. 5. The Pearson correlation matrix between the connectivity of each of the 18 AAL3 areas in the 4 ROIs with all ipsilateral AAL3 brain areas across 50 participants.

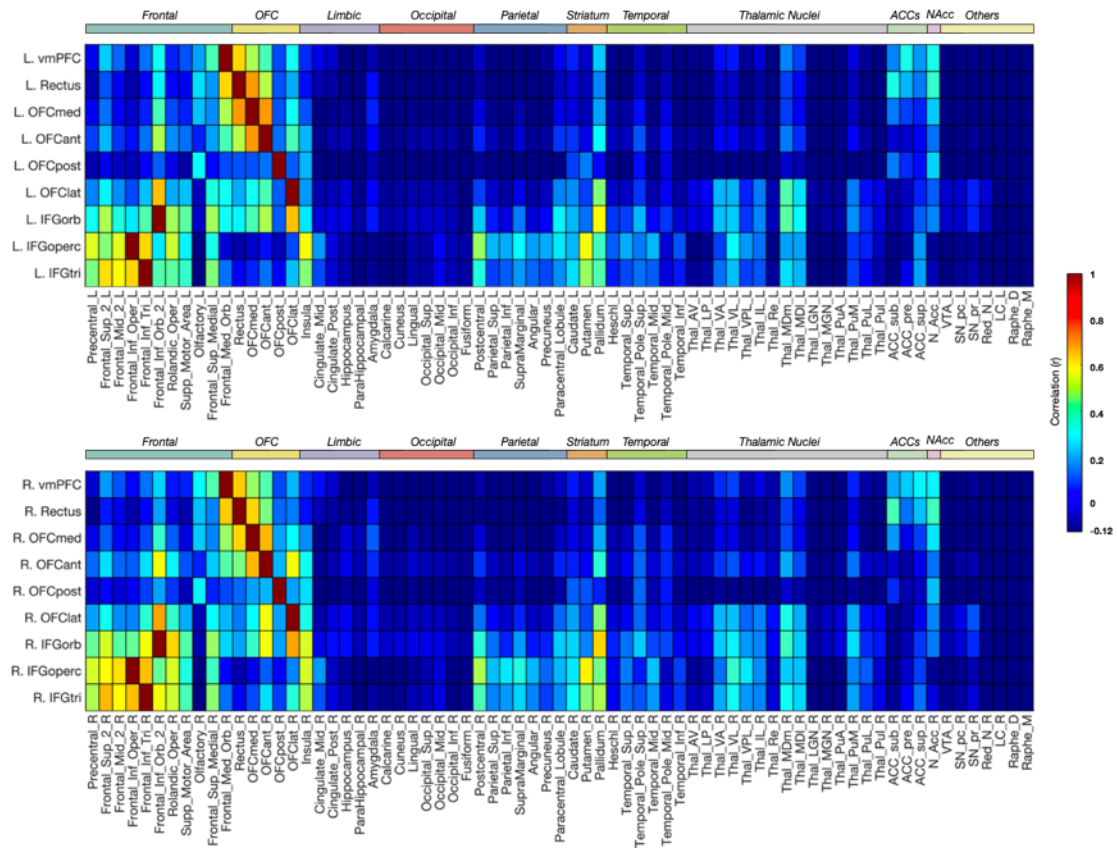
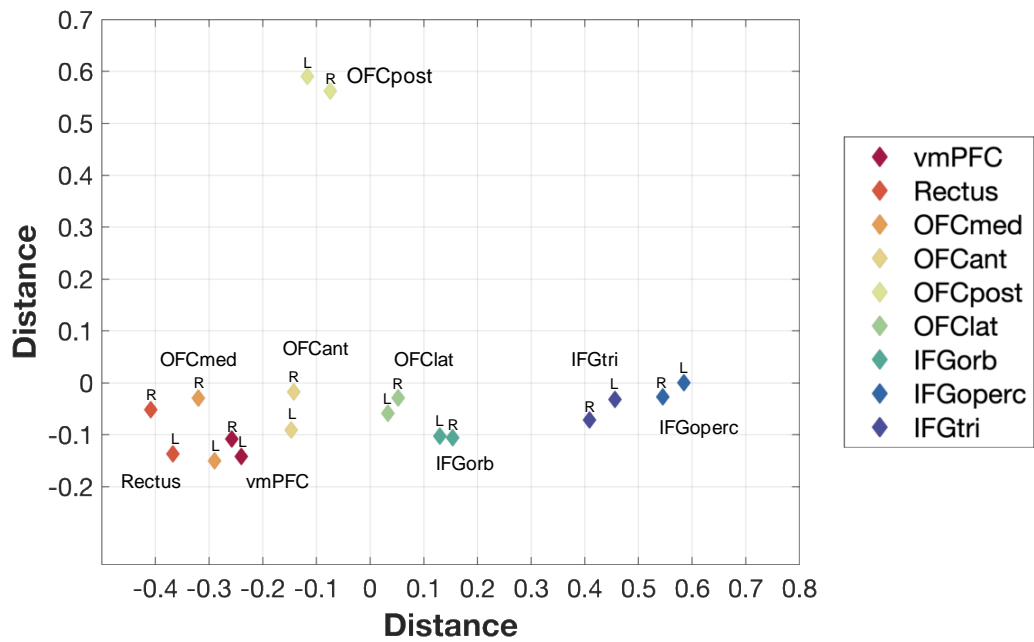


Fig. 6. Multidimensional scaling to enable visualization of the distances between the connectivity of the 18 ROIs with all AAL3 regions. The data were from the connectivity matrix shown in Fig. S2. The connections of any one ROI in this diagram with all AAL3 regions, whether on the Left or Right, are shown. The results were similar if the connections with ipsilateral AAL3 areas was used. Distances in this space reflect the dissimilarity of the connectivity.



References

- Amunts K, Zilles K. 2012. Architecture and organizational principles of Broca's region. *Trends Cogn Sci* 16:418-426.
- Barbas H. 1993. Organization of cortical afferent input to the orbitofrontal area in the rhesus monkey. *Neuroscience* 56:841-864.
- Barbas H. 2007. Specialized elements of orbitofrontal cortex in primates. *Ann N Y Acad Sci* 1121:10-32.
- Barbas H, Pandya DN. 1989. Architecture and intrinsic connections of the prefrontal cortex in the rhesus monkey. *J Comp Neurol* 286:353-375.
- Barbas H, Zikopoulos B, Timbie C. 2011. Sensory pathways and emotional context for action in primate prefrontal cortex. *Biol Psychiatry* 69:1133-1139.
- Beck E. 1949. A cytoarchitectural investigation into the boundaries of cortical areas 13 and 14 in the human brain. *J Anat* 83:147-157.
- Binder JR. 2015. The Wernicke area: Modern evidence and a reinterpretation. *Neurology* 85:2170-2175.
- Bonnici HM, Maguire EA. 2018. Two years later - Revisiting autobiographical memory representations in vmPFC and hippocampus. *Neuropsychologia* 110:159-169.
- Campbell KL, Tyler LK. 2018. Language-related domain-specific and domain-general systems in the human brain. *Curr Opin Behav Sci* 21:132-137.
- Carmichael ST, Price JL. 1995. Limbic connections of the orbital and medial prefrontal cortex in macaque monkeys. *J Comp Neurol* 363:615-641.
- Carmichael ST, Price JL. 1996. Connectional networks within the orbital and medial prefrontal cortex of macaque monkeys. *J Comp Neurol* 371:179-207.
- Catani M, Dell'acqua F, Thiebaut de Schotten M. 2013. A revised limbic system model for memory, emotion and behaviour. *Neurosci Biobehav Rev* 37:1724-1737.
- Cheng W, Rolls ET, Gu H, Zhang J, Feng J. 2015. Autism: reduced functional connectivity between cortical areas involved in face expression, theory of mind, and the sense of self. *Brain* 138:1382-1393.
- Cheng W, Rolls ET, Qiu J, Liu W, Tang Y, Huang CC, Wang X, Zhang J, Lin W, Zheng L, Pu J, Tsai SJ, Yang AC, Lin CP, Wang F, Xie P, Feng J. 2016. Medial reward and lateral non-reward orbitofrontal cortex circuits change in opposite directions in depression. *Brain* 139:3296-3309.
- Cheng W, Rolls ET, Qiu J, Xie X, Lyu W, Li Y, Huang CC, Yang AC, Tsai SJ, Lyu F, Zhuang K, Lin CP, Xie P, Feng J. 2018a. Functional connectivity of the human amygdala in health and in depression. *Soc Cogn Affect Neurosci* 13:557-568.
- Cheng W, Rolls ET, Qiu J, Xie X, Wei D, Huang CC, Yang AC, Tsai SJ, Li Q, Meng J, Lin CP, Xie P, Feng J. 2018b. Increased functional connectivity of the posterior cingulate cortex

- with the lateral orbitofrontal cortex in depression. *Transl Psychiatry* 8:90.
- Cheng W, Rolls ET, Qiu J, Yang D, Ruan H, Wei D, Zhao L, Meng J, Xie P, Feng J. 2018c. Functional connectivity of the precuneus in unmedicated patients with depression. *Biol Psychiatry Cogn Neurosci Neuroimaging* 3:1040-1049.
- Cheng W, Rolls ET, Ruan H, Feng J. 2018d. Functional connectivities in the brain that mediate the association between depressive problems and sleep quality. *JAMA Psychiatry* 75:1052-1061.
- Clos M, Amunts K, Laird AR, Fox PT, Eickhoff SB. 2013. Tackling the multifunctional nature of Broca's region meta-analytically: co-activation-based parcellation of area 44. *Neuroimage* 83:174-188.
- Corcoles-Parada M, Ubero-Martinez M, Morris RGM, Insausti R, Mishkin M, Munoz-Lopez M. 2019. Frontal and Insular Input to the Dorsolateral Temporal Pole in Primates: Implications for Auditory Memory. *Front Neurosci* 13:1099.
- DeWitt I, Rauschecker JP. 2013. Wernicke's area revisited: parallel streams and word processing. *Brain Lang* 127:181-191.
- Donahue CJ, Sotiropoulos SN, Jbabdi S, Hernandez-Fernandez M, Behrens TE, Dyrby TB, Coalson T, Kennedy H, Knoblauch K, Van Essen DC, Glasser MF. 2016. Using Diffusion Tractography to Predict Cortical Connection Strength and Distance: A Quantitative Comparison with Tracers in the Monkey. *J Neurosci* 36:6758-6770.
- Du J, Rolls ET, Cheng W, Li Y, Gong W, Qiu J, Feng J. 2020. Functional connectivity of the orbitofrontal cortex, anterior cingulate cortex, and inferior frontal gyrus in humans. *Cortex* 123:185-199.
- Eden AS, Schreiber J, Anwander A, Keuper K, Laeger I, Zwanzger P, Zwitserlood P, Kugel H, Döbel C. 2015. Emotion regulation and trait anxiety are predicted by the microstructure of fibers between amygdala and prefrontal cortex. *J Neurosci* 35:6020-6027.
- Folloni D, Sallet J, Khrapitchev AA, Sibson N, Verhagen L, Mars RB. 2019. Dichotomous organization of amygdala/temporal-prefrontal bundles in both humans and monkeys. *Elife* 8:e47175.
- Garcia-Cabezas MA, Barbas H. 2017. Anterior Cingulate Pathways May Affect Emotions Through Orbitofrontal Cortex. *Cereb Cortex* 27:4891-4910.
- Ghashghaei HT, Barbas H. 2002. Pathways for emotion: interactions of prefrontal and anterior temporal pathways in the amygdala of the rhesus monkey. *Neuroscience* 115:1261-1279.
- Gibbard CR, Ren J, Skuse DH, Clayden JD, Clark CA. 2018. Structural connectivity of the amygdala in young adults with autism spectrum disorder. *Hum Brain Mapp* 39:1270-1282.
- Glascher J, Adolphs R, Damasio H, Bechara A, Rudrauf D, Calamia M, Paul LK, Tranel D.

2012. Lesion mapping of cognitive control and value-based decision making in the prefrontal cortex. *Proc Natl Acad Sci U S A* 109:14681-14686.
- Grabenhorst F, Rolls ET. 2011. Value, pleasure, and choice in the ventral prefrontal cortex. *Trends Cogn Sci* 15:56-67.
- Greve DN, Fischl B. 2009. Accurate and robust brain image alignment using boundary-based registration. *Neuroimage* 48:63-72.
- Haber SN. 2016. Corticostriatal circuitry. *Dialogues Clin Neurosci* 18:7-21.
- Haber SN, Kunishio K, Mizobuchi M, Lynd-Balta E. 1995. The orbital and medial prefrontal circuit through the primate basal ganglia. *J Neurosci* 15:4851-4867.
- Hof PR, Mufson EJ, Morrison JH. 1995. Human orbitofrontal cortex: cytoarchitecture and quantitative immunohistochemical parcellation. *J Comp Neurol* 359:48-68.
- Hornak J, O'Doherty J, Bramham J, Rolls ET, Morris RG, Bullock PR, Polkey CE. 2004. Reward-related reversal learning after surgical excisions in orbitofrontal and dorsolateral prefrontal cortex in humans. *J Cogn Neurosci* 16:463-478.
- Jenkinson M, Bannister P, Brady M, Smith S. 2002. Improved optimization for the robust and accurate linear registration and motion correction of brain images. *Neuroimage* 17:825-841.
- Jenkinson M, Smith S. 2001. A global optimisation method for robust affine registration of brain images. *Med Image Anal* 5:143-156.
- Jeurissen B, Descoteaux M, Mori S, Leemans A. 2019. Diffusion MRI fiber tractography of the brain. *NMR Biomed* 32:e3785.
- Jeurissen B, Tournier JD, Dhollander T, Connelly A, Sijbers J. 2014. Multi-tissue constrained spherical deconvolution for improved analysis of multi-shell diffusion MRI data. *Neuroimage* 103:411-426.
- Johansen-Berg H, Behrens TE, Sillery E, Ciccarelli O, Thompson AJ, Smith SM, Matthews PM. 2005. Functional-anatomical validation and individual variation of diffusion tractography-based segmentation of the human thalamus. *Cereb Cortex* 15:31-39.
- Johansen-Berg H, Gutman DA, Behrens TE, Matthews PM, Rushworth MF, Katz E, Lozano AM, Mayberg HS. 2008. Anatomical connectivity of the subgenual cingulate region targeted with deep brain stimulation for treatment-resistant depression. *Cereb Cortex* 18:1374-1383.
- McCormick C, Ciaramelli E, De Luca F, Maguire EA. 2018. Comparing and Contrasting the Cognitive Effects of Hippocampal and Ventromedial Prefrontal Cortex Damage: A Review of Human Lesion Studies. *Neuroscience* 374:295-318.
- Mori S, van Zijl PC. 2002. Fiber tracking: principles and strategies - a technical review. *NMR Biomed* 15:468-480.
- Nasreddine ZS, Phillips NA, Bedirian V, Charbonneau S, Whitehead V, Collin I, Cummings JL, Chertkow H. 2005. The Montreal Cognitive Assessment, MoCA: a brief

- screening tool for mild cognitive impairment. *J Am Geriatr Soc* 53:695-699.
- Öngür D, Ferry AT, Price JL. 2003. Architectonic division of the human orbital and medial prefrontal cortex. *J Comp Neurol* 460:425-449.
- Passingham REP, Wise SP. 2012. *The Neurobiology of the Prefrontal Cortex*. Oxford: Oxford University Press.
- Patterson K, Nestor PJ, Rogers TT. 2007. Where do you know what you know? The representation of semantic knowledge in the human brain. *Nat Rev Neurosci* 8:976-987.
- Petrides M, Pandya DN. 1988. Association fiber pathways to the frontal cortex from the superior temporal region in the rhesus monkey. *J Comp Neurol* 273:52-66.
- Price JL. 2006. Connections of orbital cortex. In: Zald DH, Rauch SL, editors. *The Orbitofrontal Cortex*. Oxford: Oxford University Press p 39-55.
- Price JL. 2007. Definition of the orbital cortex in relation to specific connections with limbic and visceral structures and other cortical regions. *Ann N Y Acad Sci* 1121:54-71.
- Reveley C, Seth AK, Pierpaoli C, Silva AC, Yu D, Saunders RC, Leopold DA, Ye FQ. 2015. Superficial white matter fiber systems impede detection of long-range cortical connections in diffusion MR tractography. *Proc Natl Acad Sci U S A* 112:E2820-2828.
- Rizzo G, Milardi D, Bertino S, Basile GA, Di Mauro D, Calamuneri A, Chillemi G, Silvestri G, Anastasi G, Bramanti A, Cacciola A. 2018. The Limbic and Sensorimotor Pathways of the Human Amygdala: A Structural Connectivity Study. *Neuroscience* 385:166-180.
- Rolls ET. 2014. *Emotion and Decision-Making Explained*. Oxford: Oxford University Press.
- Rolls ET. 2016a. *Cerebral Cortex: Principles of Operation*. Oxford: Oxford University Press.
- Rolls ET. 2016b. A non-reward attractor theory of depression. *Neurosci Biobehav Rev* 68:47-58.
- Rolls ET. 2018. The storage and recall of memories in the hippocampo-cortical system. *Cell Tissue Res* 373:577-604.
- Rolls ET. 2019a. The cingulate cortex and limbic systems for emotion, action, and memory. *Brain Struct Funct* 224:3001-3018.
- Rolls ET. 2019b. *The Orbitofrontal Cortex*. Oxford: Oxford University Press.
- Rolls ET. 2019c. The orbitofrontal cortex and emotion in health and disease, including depression. *Neuropsychologia* 128:14-43.
- Rolls ET. 2021. *Brain Computations: A Systems-Level Analysis*. Oxford: Oxford University Press.
- Rolls ET, Cheng W, Du J, Wei D, Qiu J, Dai D, Zhou Q, Xie P, Feng J. 2020a. Functional connectivity of the right inferior frontal gyrus and orbitofrontal cortex in depression. *Soc Cogn Affect Neurosci* 15:75-86.

- Rolls ET, Cheng W, Gong W, Qiu J, Zhou C, Zhang J, Lv W, Ruan H, Wei D, Cheng K, Meng J, Xie P, Feng J. 2019. Functional connectivity of the anterior cingulate cortex in depression and in health. *Cereb Cortex* 29:3617-3630.
- Rolls ET, Grabenhorst F. 2008. The orbitofrontal cortex and beyond: from affect to decision-making. *Prog Neurobiol* 86:216-244.
- Rolls ET, Grabenhorst F, Deco G. 2010a. Choice, difficulty, and confidence in the brain. *Neuroimage* 53:694-706.
- Rolls ET, Grabenhorst F, Deco G. 2010b. Decision-making, errors, and confidence in the brain. *J Neurophysiol* 104:2359-2374.
- Rolls ET, Huang CC, Lin CP, Feng J, Joliot M. 2020b. Automated anatomical labelling atlas 3. *Neuroimage* 206:116189.
- Rolls ET, Joliot M, Tzourio-Mazoyer N. 2015. Implementation of a new parcellation of the orbitofrontal cortex in the automated anatomical labeling atlas. *Neuroimage* 122:1-5.
- Saleem KS, Kondo H, Price JL. 2008. Complementary circuits connecting the orbital and medial prefrontal networks with the temporal, insular, and opercular cortex in the macaque monkey. *J Comp Neurol* 506:659-693.
- Saleem KS, Miller B, Price JL. 2014. Subdivisions and connectional networks of the lateral prefrontal cortex in the macaque monkey. *J Comp Neurol* 522:1641-1690.
- Selemon LD, Goldman-Rakic PS. 1985. Longitudinal topography and interdigitation of corticostriatal projections in the rhesus monkey. *J Neurosci* 5:776-794.
- Smith RE, Tournier JD, Calamante F, Connelly A. 2012. Anatomically-constrained tractography: improved diffusion MRI streamlines tractography through effective use of anatomical information. *Neuroimage* 62:1924-1938.
- Smith SM. 2002. Fast robust automated brain extraction. *Hum Brain Mapp* 17:143-155.
- Solano-Castiella E, Anwender A, Lohmann G, Weiss M, Docherty C, Geyer S, Reimer E, Friederici AD, Turner R. 2010. Diffusion tensor imaging segments the human amygdala in vivo. *Neuroimage* 49:2958-2965.
- Tournier J-D, Calamante F, Connelly A. 2010. Improved probabilistic streamlines tractography by 2nd order integration over fibre orientation distributions. *Proc Intl Soc Mag Reson Med (ISMRM)* 18:1670.
- Van Essen DC, Hayashi T, Aulio J, Ose T, Nishigori K, Coors T, Hou Y, Smith S, Shen Z, Knoblauch K, Kennedy H, Glasser M. 2019. Evaluation of functional connectivity using retrograde tracers in the macaque monkey. *Organisation for Human Brain Mapping*:https://www.pathlms.com/ohbm/courses/12238/sections/15845/video_presentations/138035.
- Wheeler EZ, Fellows LK. 2008. The human ventromedial frontal lobe is critical for learning from negative feedback. *Brain* 131:1323-1331.

Yeterian EH, Pandya DN. 1991. Prefrontostriatal connections in relation to cortical architectonic organization in rhesus monkeys. *J Comp Neurol* 312:43-67.

Zajac L, Koo BB, Bauer CM, Killiany R, Behalf Of The Alzheimer's Disease Neuroimaging I. 2017. Seed Location Impacts Whole-Brain Structural Network Comparisons between Healthy Elderly and Individuals with Alzheimer's Disease. *Brain Sci* 7:37.